THE INTERMEDIATE VELOCITY SOURCE IN THE ^{40}Ca+^{197}Au REACTION AT 35 AMeV

R. Płaneta[a], Z. Sosin[a], P. Hachaj[a], T. Ciszek[a], W. Gawlikowicz[a], K. Grotowski[a,d], S. Micek[a], P. Pawłowski[a], A.J. Cole[b], D. Benchekrounc[c], E. Bisquer[c], A. Chabane[b], M. Charvet[b], B. Cheynis[c], A. Demeyer[c], P. Désesquelles[b], E. Gerlic[c], A. Giorni[b], D. Guinet[c], D. Heuer[b], P. Lautesse[c], L. Lebreton[c], A. Lléres, M. Stern[c], L. Vagneron[c], and J.B. Viano[b]

[a]M. Smoluchowski Institute of Physics, Jagiellonian University
Reymonta 4, 30-059 Cracow, Poland
[b]Institut des Sciences Nucléaires de Grenoble
IN2P3-CNRS/ Université Joseph Fourier
53, Avenue des Martyrs, F-38046 Grenoble Cedex, France
[c]Institut de Physique Nucléaire de Lyon
IN2P3-CNRS/ Université Claude Bernard, 43
Boulevard du 11 Novembre 1918, F-69622 Villeurbanne Cedex, France
[d]H. Niewodniczański Institute of Nuclear Physics
Radzikowskiego 152, 31-342 Cracow, Poland

(Received August 20, 2001)

The creation of hot Ca-like fragments and the emission of intermediate velocity particles was studied in the 40Ca+197Au reaction at 35 AMeV. For peripheral collisions the primary projectile-like fragment was reconstructed using the AMPHORA 4π detector system. The particle distributions are compared with the predictions of a Monte Carlo code which calculates the nucleon transfer and clustering probabilities according to the system density of states. The velocity distributions of charged particles projected on the beam direction can be explained if emissions from the hot projectile-like fragment and the target-like fragment are supplemented by an emission from an intermediate velocity source located between them. The properties of the intermediate velocity source are properly described, including the ^{2}D/^{3}T/^{3}He effect.

PACS numbers: 25.70.Gh, 25.70.Lm, 25.70.Pq

1. Introduction

In heavy ion collisions at low and intermediate energies nucleons are exchanged between the reaction partners, and "hot sources" of particles are created as a result of energy dissipation. These "hot sources" are frequently used as a test ground for nuclear thermodynamics [1]. The number and properties of these "hot sources" depend very much on the collision energy. At low energies one observes the emission of Light Particles (LPs) evaporated from the Compound System (CS) (small impact parameters) or from the Projectile-Like Fragment (PLF), and the Target-Like Fragment (TLF) produced in Deep Inelastic Collisions (DICs) [2]. At higher energies, new "hot sources" appear in succession: pre-equilibrium "sources", intermediate velocity "sources" (IVSs), or mid-rapidity "sources" [3]. The LP emission is here gradually supplemented by the production of intermediate mass fragments (IMFs) with atomic numbers $Z > 2$ [4]. The relative strengths of these various "sources" change with increasing energy. The PLF and TLF "sources" dominate at lower energies. At high energies the PLF and the TLF change into relatively low-excited spectators, while the overlap zone between the colliding ions becomes most active [5]. The collision energy determines likewise the reaction mechanism. For lower energies, a di-nuclear system is briefly formed. Its shape changes with time and depends on the surface tension, the Coulomb, and the centrifugal forces. The effective flow of nucleons between the projectile and the target nucleus is governed by the mean field, but fluctuations may also be important [6]. Energy damping in the system before break-up is the product of one-body dissipation [7]. At high energies the Pauli principle is much less effective in restricting the Nucleon-Nucleon (NN) collisions in the overlap zone of the interacting heavy ions, and the dissipation of energy has mainly a two-body character.

The intermediate velocity "sources", primarily suggested by BUU [8] and BNV [9,10] calculations, have been observed in some number of experiments. This observation is done by a reconstruction–subtraction procedure [11], by inspecting the shapes of the velocity distributions of charged particles projected on the beam direction [12], by inspecting invariant velocity plots [9,13,14] or rapidity and transversal energy distributions [15,16], or by observing the so-called "aligned breakup" [17]. A more complete list of references can be found in [12]. In spite of all these efforts, neither the properties nor the nature of the IVS is well understood. According to different sets of data, the IVSs decay primarily by emitting IMSs [9,11,13,14], or IMSs and LPs [11,13–16]. A preferential emission of tritons and a suppressed emission of ^{3}He ions (the so-called ^{3}T/^{3}He anomaly) has been suggested [11–15].

Different scenarios and models have been used in order to describe the IVS creation and decay: the dynamic fragmentation of a neck zone between the reaction partners [13,14], a coalescence model coupled to the ISABEL intra-cascade code [18], the molecular dynamics model [11], or a stochastic model of nucleon transfer [12].

It is not an easy task to observe and describe the properties of the PLF, the TLF, and the intermediate velocity "sources". The difficulties are not only theoretical but also experimental in nature. Due to the high multiplicity and diversity of the particles emitted, the experimental investigation of heavy ion reactions in the intermediate energy region requires high granularity 4π multi-detector systems and special filters to select various particle "sources". The particles, especially light particles, emitted by different "sources" overlap in the velocity (momentum) space, which may be observed in the invariant velocity plots. In this situation it would be very helpful to have a model which properly reproduces the overall reaction picture and may be used to distinguish the particles emitted from different "sources".

This was the case of the ^{40}Ca+^{40}Ca reaction studied recently at 35 AMeV. A 4π multidetector system was used to reconstruct the primary projectile-like fragment (Płaneta *et al.* [19]) and identify the "source" of intermediate velocity particles (Sosin *et al.* [12]). The experimental data were quite well reproduced by the predictions of a model (Monte Carlo code PIRAT) proposed by Sosin [20], describing a heavy ion collision as a stochastic process. This code could be used to evaluate the validity of the reconstruction procedure and efficiency of the IVS separation. The shapes of the energy spectra of particles from PLF decay were found to be consistent with a thermalized "source" picture. The forward–backward symmetry of the angular distribution observed in the frame of the reconstructed PLF also suggested some sort of "loss of memory". The properties of the intermediate velocity source observed in this reaction were properly described, including the isotopic composition of the emitted particles.

The aim of the present work is to investigate the mechanism of the ^{40}Ca+^{197}Au reaction at 35 AMeV, in the vicinity of the Fermi energy. In this energy range individual NN collisions and residual Pauli blocking are expected to be important, as well as mean field effects. In particular, we would like to study the formation of the intermediate velocity source. A description of the ^{40}Ca+^{197}Au experiment and of the PLF reconstruction procedure is presented in Section 2. The Monte Carlo code used in this work is briefly described in Section 3. The experimental data is compared with the model's predictions in Section 4. The final section contains a summary and conclusions.

2. The ^{40}Ca+^{197}Au experiment

The experiment was carried out at the SARA facility in Grenoble. A 1.4 GeV Ca beam was focused on a 0.5 mg/cm^2 Au target located inside an AMPHORA detector system [21], which covers about 80% of 4π. In addition to the standard AMHORA detectors, 30 gas ionization chambers were placed in front of the CsI detectors, instead of thin scintillator foils. This was done for two detector rings at 31.2 and 46.6 degrees LAB [22], lowering the energy thresholds to about 1 AMeV. The elastic scattering of ^{4}He, ^{12}C, ^{16}O, and ^{20}Ne ions at four different energies was used to calibrate the IMF energy. The detector system could identify charge and mass numbers of light particles, and only charge numbers of IMFs.

The total kinetic energy of the detected particles, which is important for the reconstruction procedures, may be influenced by random coincidences [23]. To avoid this effect, no on-line multiplicity triggers were applied, and low beam intensity was used. In addition, windows were set on the time spectra in order to clean out data from accidental coincidences coming from different beam bursts.

In order to obtain a reasonable reconstruction of the Ca-like fragments, events with a sufficiently high measured value of total parallel momentum ($p_{\mathrm{par}} > 8\,\mathrm{GeV}/c$) were selected as "well" defined and used for further analysis.

The PLF reconstruction procedure (see [3] and [19]) begins by constructing, for each event, the velocity vector of the primary PLF from the momentum vectors of the products. We use here the CM velocity of fragments with $Z \geq Z_{\mathrm{min}} = 3$ and require their velocities to be larger than one half of the projectile LAB velocity. This procedure minimizes possible contamination from sources other than the PLF.

In the next step the primary PLF charge is calculated as the sum of the charges of the detected particles. All $Z \geq Z_{\mathrm{min}} = 3$ particles were taken for which the parallel velocity component in the rest frame of the primary PLF is larger than minus 0.1c. For LPs, the emission in the backward hemisphere overlaps with the emission from other sources. As in the analysis of the ^{40}Ca+^{40}Ca reaction, only particles emitted in the forward hemisphere were taken for $Z < Z_{\mathrm{min}}$, and their number was multiplied by two. In this way we minimize the contribution of light particles coming from other sources.

For the ^{40}Ca+^{40}Ca reaction, in order to estimate the primary PLF mass, a mass A_{IMF}, equal to $2Z_{\mathrm{IMF}}$ was assumed for each IMF. For those particles for which $Z < Z_{\mathrm{min}}$ the measured masses of all the fragments emitted in the forward hemisphere were summed up and multiplied by two. It was also assumed that in each event the number of emitted neutrons, N_{neutron}, is equal to the number of emitted protons, N_{proton}. As will be shown in Section 3, in the case of the ^{40}Ca+^{197}Au reaction this approximation is not justified and a correction is necessary.

The calorimetric method is used to estimate the excitation energy. The kinetic energies of the fragments in the rest frame of the PLF are summed up with the same restrictions as for the reconstruction of charge and mass. The contribution of light particles ($Z < Z_{\rm min}$) emitted in the forward hemisphere is multiplied by two. The sum of the kinetic energy of the neutrons is assumed to be equal to that of the protons, plus correction, and minus the Coulomb energy. Finally, we include the relevant Q value, estimated by using particle masses.

As discussed in Section 1, the heavy ion reaction mechanism depends on the entrance channel angular momentum L (collision parameter). The angular momentum is not experimentally measurable; instead, we have used here the total transversal momentum, $p_{\rm tr}$, of the charged particles detected. The $p_{\rm tr}$ *versus* L dependence is monotonic but considerably diffused (see Fig. 1). As a result, the $p_{\rm tr}$ window contains quite a broad range of different L values. Nevertheless, $p_{\rm tr}$ can be used as a rough measure of the total dissipated energy. Most of the events shown in Fig. 1 are located in the region of larger L values due to a cutoff introduced by the $p_{\rm par} > 8{\rm GeV}/c$ condition. Therefore our investigation is limited to a region of more peripheral collisions.

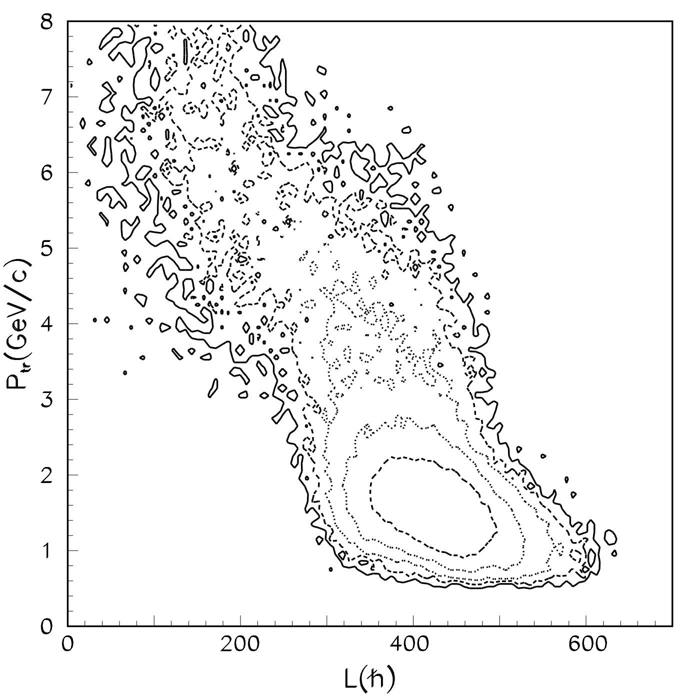

Fig. 1. The dependence $p_{\rm tr}$ *vs* L; model prediction.

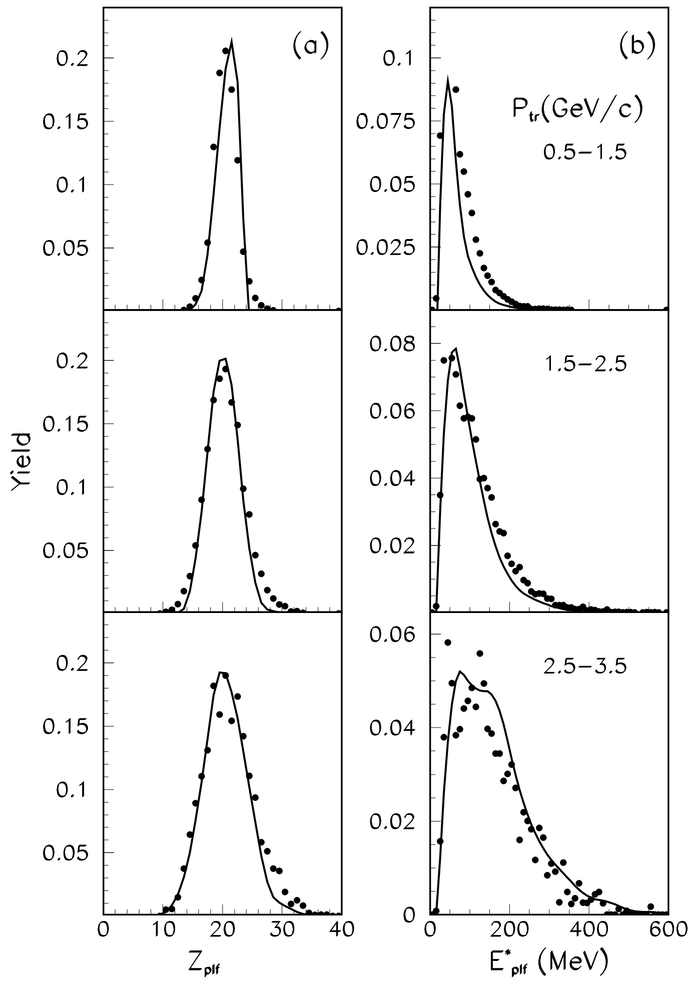

Fig. 2. Charge (a), and excitation energy (b) distributions of the reconstructed PLF for consecutive $p_{\rm tr}$ windows. Experimental points and model predictions.

The distribution of the reconstructed PLF charge, $Z_{\rm PLF}$, is presented in Fig. 2(a), for consecutive $p_{\rm tr}$ windows. All distributions are centered around $Z_{\rm PLF} = 20$, which implies that in the region of more peripheral collisions the same number of protons (on the average) is transferred from and to the Ca projectile. The width of the $Z_{\rm PLF}$ distribution increases slightly with the $p_{\rm tr}$, which is partly induced by the reconstruction procedure.

The reconstructed PLF excitation energy distributions ($E^*_{\rm PLF}$)are shown in Fig. 2(b) for the same $p_{\rm tr}$ windows. The distributions become broader for more central collisions and the primary average PLF excitation energy increases.

Figs. 3 and 4 display the velocity distributions of charged particles projected on the beam direction. In our experiment the He isotopes were properly separated only at higher energies. Therefore, for helium3 particles we present the higher velocity part of the v_z distribution. The intensity of alpha particles is much higher than of helium3 particles, and therefore the helium3 contamination of the low velocity alpha particle spectra can be ignored.

The p, ^{3}He, α, and Ne velocity distributions in Fig. 3 (no restrictions imposed on the $p_{\rm tr}$ values) are characterized by a maximum placed above 0.2 c, in the region of the PLF velocities. For deuterons and tritons this maximum is shifted towards smaller velocities. For more peripheral collisions (Fig. 4, $p_{\rm tr} < 1.5$ GeV$/c$) the maximum observed in the deuteron and triton velocity distributions becomes narrower. It could be supposed that most of the deuterons and tritons are emitted not from the PLF "source", but from the IVS. In order to ascertain if such a conjecture is justified, we will compare the experimental data with the predictions of the model presented in Section 3.

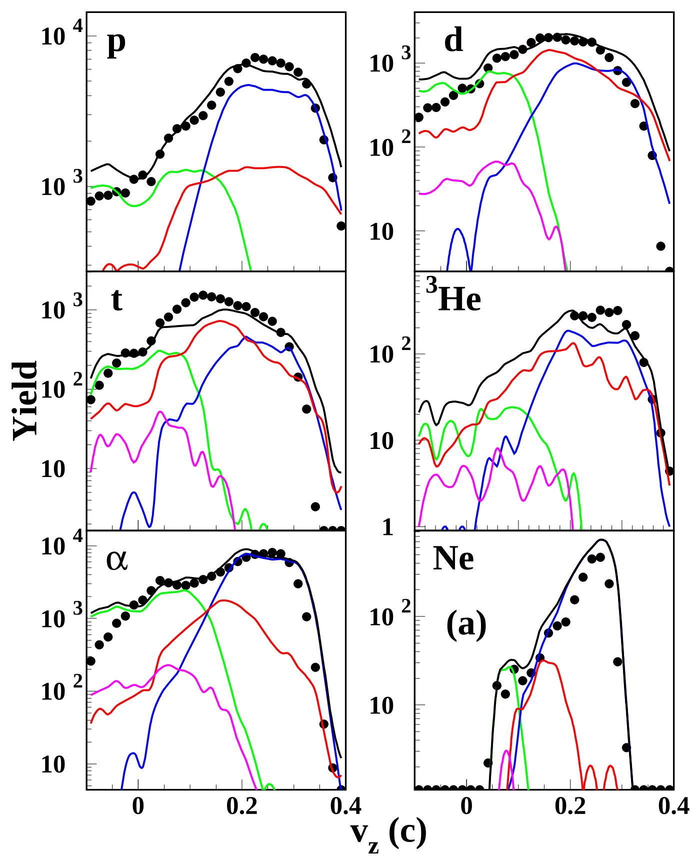

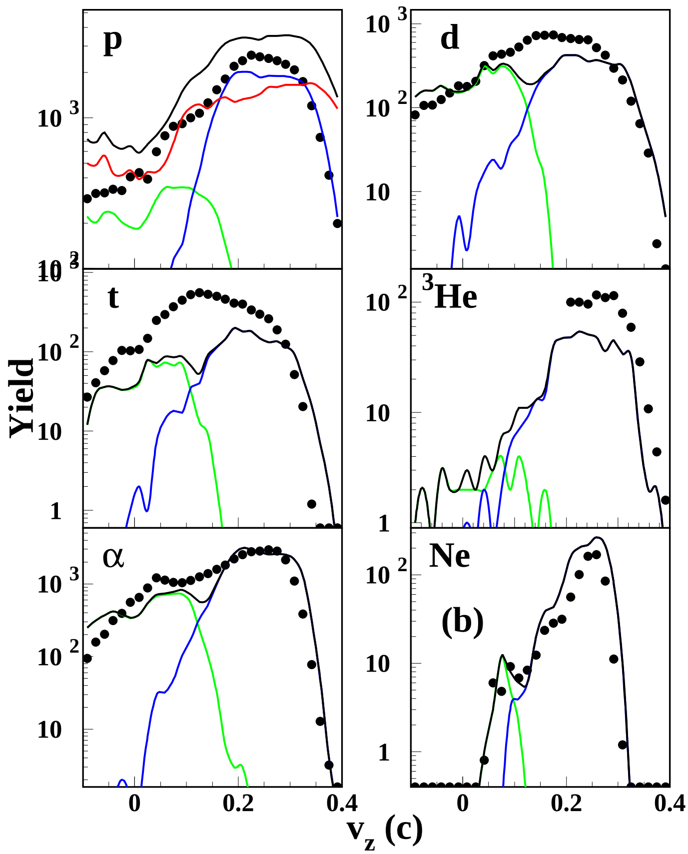

Fig. 3. Velocity (v_z) distributions (LAB) projected on a direction parallel to the beam; black dots: experimental data. Model predictions for IVS, PLF, and TLF sources: red, blue, and green lines, respectively. Black line: predicted total emission. Violet line: CS contribution. Three "source" calculations (a); two source calculations (b).

3. The Monte Carlo model

The stochastic model (PIRAT code [20]) used in this work describes a heavy ion collision as a two-stage process. Some of the nucleons become reaction participants in the first stage by mean field effects or by nucleon-nucleon (NN) interactions and are transferred in the second stage to the target remnant, or to the projectile remnant. Alternatively, they may form clusters located in the region between colliding Ca ions, or escape to the

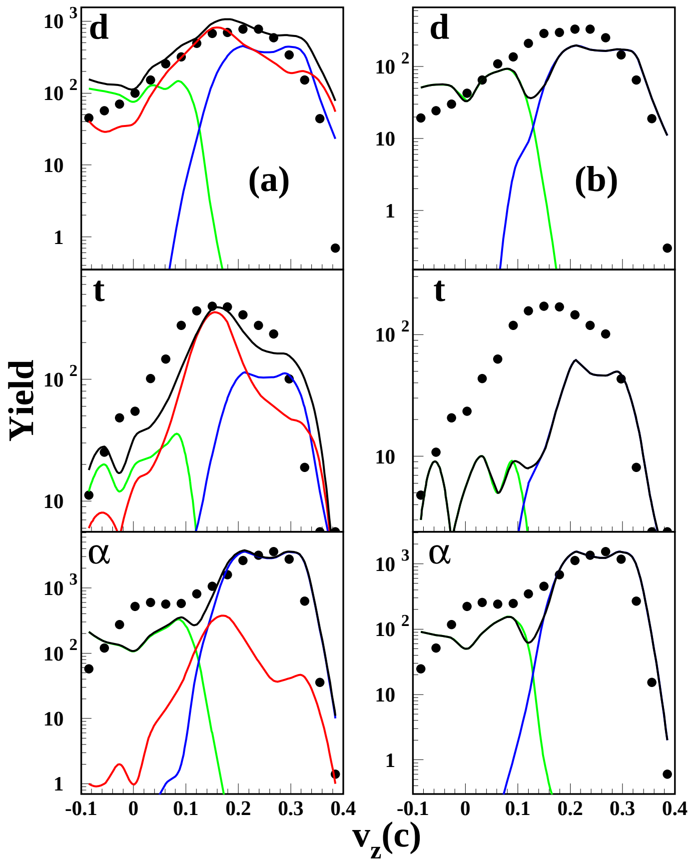

Fig. 4. Velocity (v_z) distributions (LAB) of deuterons, tritons, and alphas for $p_{\rm tr} < 1.5$ GeV/c. Model prediction and experimental points. Three "source" calculations (a); two source calculations (b). The key for the lines is the same as in Fig. 3.

continuum. The nucleon transfer probabilities are governed by the state densities. The various hot fragments created in this way afterwards decay by particle emission, which is simulated by the GEMINI code [24]. Clusters and other final fragments (particles) are accelerated by Coulomb forces. After the formation of all the fragments, the PLF and TLF may fuse. This happens when due to the dissipation of energy and relative angular momentum a "pocket" appears in the PLF–TLF interaction potential and the energy of the system is smaller than the potential barrier. A detailed description of the model may be found in [20].

For purposes of comparison with the experimental data, the model predictions are filtered by a software replica of the AMPHORA detector.

A. First stage — mean field mechanism

In the mean field mechanism some of the nucleons of the projectile nucleus (P) and of the Target nucleus (T) become reaction participants when run across a potential window which opens in the region between the colliding heavy ions. The degree and duration of opening depends on the proximity and relative velocity of the heavy ions on their classical trajectories, calculated for the Coulomb plus proximity potential. By using parabolic approximation (see, *e.g.*, Tassan–Got and Stéphan [25]) one obtains the values of the potential barrier transmission probability across the window. For each heavy ion impact parameter, bHI, the number of participating nucleons is obtained by a Monte Carlo procedure from the Poisson distribution around $\langle n_{cr} \rangle$, the average number of nucleons per event crossing the potential window.

B. First stage — two-nucleon mechanism

In the NN mechanism two nucleons, one from the projectile (P) and the other from the target (T), collide in the overlap zone of the P and T nuclei, where for larger collision energies and/or larger collision parameters the Pauli principle becomes less restrictive. The nucleons of such a pair become reaction participants. The probability of an NN collision depends on the NN interaction cross-section, the convolution of the P and T densities in the overlap region, and the available momentum space.

For a given b_{HI} and with no Pauli blocking, the average number of NN collisions per event, $\langle n_{i,j} \rangle$, is calculated in the modified optical limit of the Glauber theory [26], along the heavy ion trajectory in the entrance channel potential. Here i, j denotes n (neutron) or p (proton), respectively. The distribution of $n_{i,j}$ is given by the NN collision probability P_{ij}, calculated for all pairs of nucleons, and for the Pauli blocking effect checked each time. The P_{ij}'s dependence on the NN collision parameter is parameterized as Gaussian. The parameters of this distribution depend on the collision parameter and on the NN cross-sections (see [20]).

The relative contribution of the mean field (one-body) mechanism and of the two-nucleon (two-body) mechanism depends on the heavy ion collision energy, the impact parameter, and the composition of heavy ions. For our reaction at 35 AMeV, this amounted to an average of 33 percent and 67 percent, respectively.

C. Second stage — nucleon transfer

In the PIRAT code, the nucleon transfer is treated as a stochastic process in which a participating nucleon may chose different options. These are as follows:

(i) re-creation of the bond with the mother nucleus; or

(ii) creation of a bond with the other nucleus, another participating nucleon, or a cluster of participating nucleons produced in an earlier step.

The nucleon transfer process is governed by a thermodynamic probability:

$$\Omega = \Delta\Omega_{\rm PR} \times \Delta\Omega_{\rm TR} \times \Delta\Omega_{\rm NFG} \times \prod_{\rm (all\,CL)} [\Delta\Omega_{\rm CL}] \times \Delta\Omega_{\rm CL,N}({\rm tr}) \times \Delta\Omega_{\rm PR,TR}({\rm tr})\,. \tag{1}$$

Here, for internal degrees of freedom, $\Delta\Omega_{\rm PR}$, $\Delta\Omega_{\rm TR}$, $\Delta\Omega_{\rm CL}$, and $\Delta\Omega_{\rm NFG}$ denote the density of states of the projectile remnant, target remnant, cluster, and "gas" of participating nucleons, respectively. The degrees of freedom corresponding to the translational motion of the system of clusters and nucleons which already left the nucleon "gas", and of the target remnant and projectile remnant, are represented by the density of states $\Delta\Omega_{\rm CL,N}({\rm tr})$, and $\Delta\Omega_{\rm PR,TR}({\rm tr})$, respectively.

In the model, the nucleon transfer process is executed in a chain of steps. A detailed description of this procedure can be found in [20].

The summation of the ground state and kinetic energies of fragments with their interaction potentials provides a value for total energy corresponding to the internal degrees of freedom (excitation energy) of the system. After subtracting the total excitation energy of the particular nucleon transfer, one obtains the corresponding reaction Q value. The total energy of the system is conserved along the chain of transfers, but the excitation energies of particular subsystems vary according to the particular Q value. This Q energy is divided among all the involved subsystems having masses $A > 4$, with a probability proportional to the corresponding densities of states.

The angular momenta and spins of the final reaction products are calculated from the initial P (or P remnant) and T (or T remnant) angular momenta, and from the angular momenta of the participating nucleons involved. For the P and T spins the model assumes zero values. In order to calculate the angular momenta of the participating nucleons we assume that their momenta are distributed as in a Fermi gas, and that the initial locations depend upon the mean field and the NN interaction mechanism.

It is assumed that the participating nucleon may join a PR, a TR, or a cluster, if:

(i) the spin of the final system (nucleus or cluster) is smaller than the maximum spin permitted for that system,

(ii) the captured nucleon's relative angular momentum is smaller than a specified critical value L_{cr}. This condition determines the value of the maximum momentum of a nucleon which can be captured by a nucleus.

It should be stressed that although on the average the nucleon transfer and the cluster coalescence process are governed by the maximum value of entropy, its fluctuations are also significant.

4. Comparison of the experimental data with the model predictions

As shown in Figs. 2(a) and 2(b), the primary Z_{PLF} and E^*_{PLF} distributions are quite well reproduced by the model predictions.

A comparison between the model predictions and the experimental data can also be estimated in Figs. 3(a) and 4(a) for the v_z velocity distributions. The model predictions generated for the IVS, and for the PLF and TLF "sources", filtered by the software replica of the AMPHORA detector [27], are presented by red, blue, and green lines, respectively. The black line describes the total emission from all sources, while the violet line traces emissions from the Composite System (CS) created in complete or incomplete fusion. The same factor was used to normalize the model predictions in reference to the experimental data. The level of agreement achieved between experimental points and the black line (total emission) is satisfactory. For deuterons, tritons and alpha particles, all three "sources" (PLF, IVS, and TLF) contribute significantly to the total emission, but to a different extent. For tritons and deuterons, IVS emission dominates. Alphas are preferentially emitted from the PLF "source", and IVS emission is in second place. For heavier ejectiles, such as Ne ions, the IVS and TLF emissions gradually disappear. However, one should bear in mind that because of the reaction kinematics and the geometry of the AMPHORA detector, the PLF emission is artificially intensified. The dominance of the IVS emission in the triton and deuteron velocity spectra is enhanced for very peripheral collisions (Fig. 4(a)). The deuteron maximum is broader than the triton, because given the same cluster gas temperature the lighter deuterons must be faster.

In order to check the hypothesis of three "sources", the model calculations have been repeated with a condition excluding the formation of clusters. It is clear (see Figs. 3(b) and 4(b)) that with this restriction the model is no longer able to describe the experimental data. For deuterons and heavier particles two maxima appeared in the model predictions, which is not consistent with experimental data. The exclusion of clusters resulted in the over-production of protons emitted from the mid-velocity region and different relative contributions of the PLF and TLF "sources".

The real relative contribution of the IVS "source" in emission of different ejectiles (model prediction, no experimental limitations) is presented in Fig. 5 for the ^{40}Ca+^{197}Au reaction (a), and also for the ^{40}Ca+^{40}Ca reaction (b). The IVS contribution is given as a percent of the total emission, for peripheral collisions taking place above some threshold angular momentum. Three values of the threshold angular momentum are considered: L_1, L_2, and L_3. For L_1, the entrance channel cross-section $\sigma(L)$ reaches its maximum value; $\sigma(L_2) = \sigma(L_3) = 0.5\sigma(L_1)$; $L_2 > L_1$ (more peripheral collisions), $L_3 < L_1$(less peripheral collisions). For the ^{40}Ca+^{197}Au reaction: $L_1 = 460\,\hbar$, $L_2 = 517\,\hbar$, $L_3 = 240\,\hbar$. For ^{40}Ca+^{40}Ca: $L_1 = 220\,\hbar$, $L_2 = 250\,\hbar$, $L_3 = 110\,\hbar$. As can be seen in Fig. 6, deuterons, tritons and ^{3}He particles are preferentially emitted in peripheral collisions by the IVS, and the IVS emission of more neutron-rich tritons and deuterons is slightly enhanced. The magnitude of this effect increases with L. The numbers of particles emitted by the IVS are small for peripheral collisions, and the error bars of the IVS contribution are quite large. There is no significant difference between the ^{40}Ca+^{197}Au and ^{40}Ca+^{40}Ca reactions. The differences between the $n_{\rm triton}/n_{\rm helium3}$ ratios (n_i denote here the respective IVS contribution) are also noteworthy. For ^{40}Ca+^{197}Au it varies between about 4 and 5, and for ^{40}Ca+^{40}Ca, between 1.4 and 1.5, for the various collision centralities considered in Fig. 5. This isospin dependence of the IVS contribution of mass 3 particles seems to be properly correlated with the N/Z ratio of the ^{40}Ca+^{197}Au and ^{40}Ca+^{40}Ca systems.

One should bear in mind that Fig. 5 presents the relative contributions of the IVS in the emission of different particles. The total charge emission and the contribution of different "sources", as seen by the AMPHORA detector, is presented in Fig. 6. The group of light particles has a flux about 25 times stronger than the flux of the IMFs, which form some kind of plateau and then peak at about $Z = 17$, just below the projectile charge. It is clear that the total charge distribution is dominated by the PLF emission. Only in the region of light particles can the IVS emission compete with the PLF emission. Fig. 6 demonstrates good agreement between the model predictions and the experimental data, up to about $Z = 20$. Some disagreement above this Z value can be explained by the appearance of Au fission, not properly described by the GEMINI code.

The question was asked in Section 2 whether the PLF reconstruction procedure used for the ^{40}Ca+^{40}Ca reaction can also be applied to the ^{40}Ca+^{197}Au reaction. As can be expected, the nucleon transfer and the cluster coalescence process depend on L (collision parameter). Fig. 7 shows how the primary PLF, TLF, IVS and CS charge depend on L. In peripheral collisions, nearly the same number of protons are transferred, in both directions (on the average), between the projectile and the target nucleus.

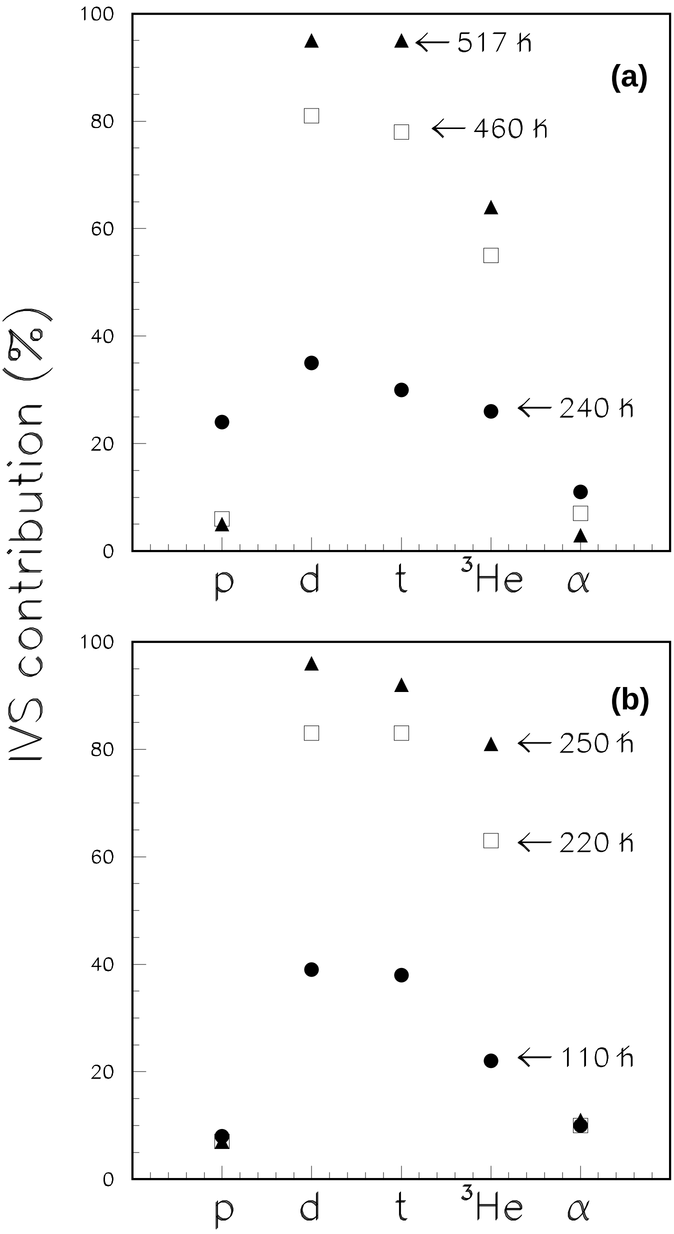

Fig. 5. Relative contribution of the IVS source in emission of different ejectiles (percent of the total emission) — model prediction with no experimental limitations. (a) ^{40}Ca+^{197}Au; (b) ^{40}Ca+^{40}Ca. Calculations performed for different angular momentum thresholds: L_1, L_2, L_3 — see text.

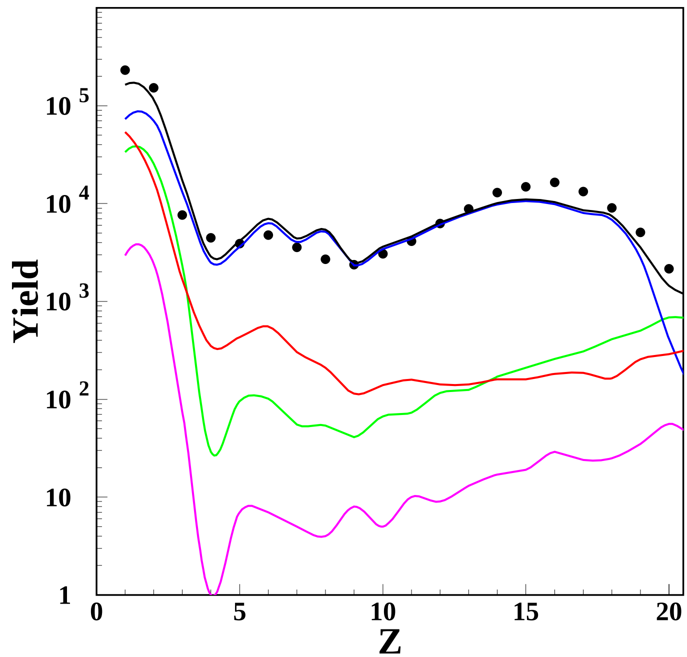

Fig. 6. Z distributions of particles emitted by different sources. Model predictions and experimental points. The key for the lines is the same as in Fig. 3.

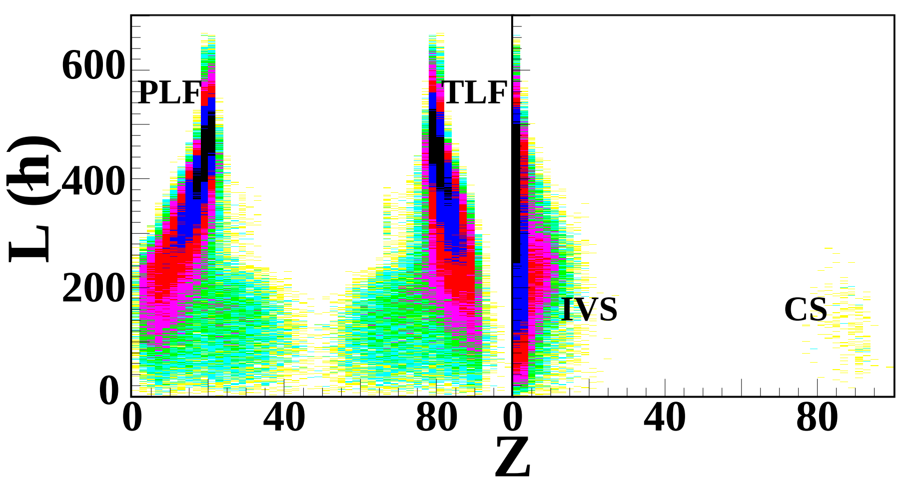

Fig. 7. The L dependence of the primary PLF, TLF, IVS and CS charge. Colors indicate different populations in the Z, L plane.

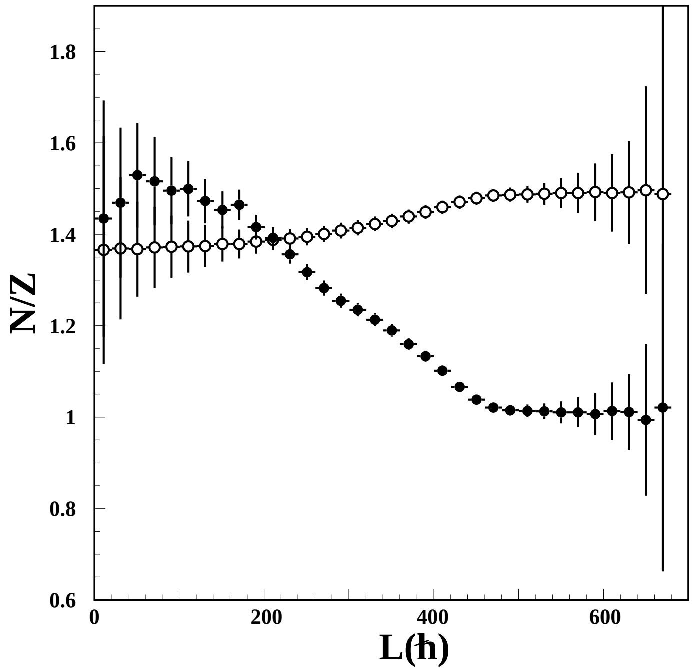

Fig. 8. N/Z *vs* L dependence for the PLF and TLF.

Some of them form the intermediate velocity source. For smaller L values, the PLF loses protons (on the average), which are transferred to the IVS and the TLF. In central collisions a composite system is created. The magnitude of the nucleon transfer is generally not the same for the neutrons and the protons. For peripheral collisions, the PLF and the TLF N/Z ratio (N denotes the neutron number) is nearly the same as that of the P and T nuclei, respectively (see Fig. 8). However, we use p_{tr} to estimate the collision centrality, and the p_{tr} *versus* L dependence is quite diffuse(see Fig. 1). As a result, a small monotonic correction is necessary (about 10 percent for the maximum value of p_{tr}) for the reconstruction of mass and excitation energy.

5. Summary and conclusions

The creation of hot Ca-like fragments and the emission of intermediate velocity particles has been observed in the ^{40}Ca+^{197}Au reaction at 35 AMeV. Because of the reaction kinematics and due to a cutoff introduced by the $p_{\mathrm{par}} > 8\,\mathrm{GeV}/c$ condition, our investigation was limited to a region of more peripheral collisions.

The general reaction picture was found to be similar to that recently studied in the ^{40}Ca+^{40}Ca reaction. The charge and excitation energy distributions of the primary PLFs were determined. The shape of the energy spectra of particles from the PLF decay is consistent with a thermalized source picture. It has been demonstrated that the charge distributions of emitted particles, and the particle velocity distributions projected on the beam direction, can be represented by the emission of particles from three "sources", the PLF, the TLF and the IVS. In particular, the shape of the particle velocity distributions cannot be properly explained without the intermediate velocity "source".

The origin and observed properties of the PLF and the IVS are properly described by the stochastic transfer and coalescence process of nucleons liberated in the heavy ion collision [20]. The "hot" PLF and TLF are created as a result of energy dissipation during the nucleon transfer process. The intermediate velocity source can be considered as a multi-component gas of nucleons and clusters of different degree of excitation. This system separates afterwards under the influence of Coulomb forces.

The yield of particles emitted from the IVS decreases with the increasing value of particle Z. Most of these are light particles. In the more peripheral collisions studied in this work, deuterons, tritons, and to lesser extent helium3 particles are preferentially emitted from the IVS. The dominance of the deuteron and triton emission over the helium3 one has been clearly observed. This effect is intensified for more central collisions. The isospin dependence of the mass 3 IVS contribution should be also mentioned.

As for the properties of the IVS, the ^{40}Ca+^{197}Au and ^{40}Ca+^{40}Ca reactions are very similar. For ^{40}Ca+^{197}Au, deuterons are slightly more preferentially emitted than tritons. In the ^{40}Ca+^{40}Ca reaction the situation is opposite. Therefore, it is probably safer to speak of a deuteron/triton/helium3 anomaly, instead of a triton or triton/helium3 anomaly. It should be stressed, however, that this effect is properly described by simulations performed with the PIRAT code, which takes into account the state densities and the distribution of Q values along the chain of nucleon transfers. Various explanations of this effect have been discussed (see [12] for references), but to date no final conclusion has been reached.

There is yet another question which could be asked in connection with the ^{40}Ca+^{197}Au reaction: what is the effective "flow" of nucleons and energy partition between the colliding ions? This was discussed some time ago in connection with some lower-energy heavy ion experiments [28]. As far as we know, no satisfactory answer was found. According to the model simulations (see Section 4) in peripheral ^{40}Ca+^{197}Au collisions, nearly the same number of protons are transferred, in both directions between the projectile and the target nucleus. For smaller L values, the PLF looses protons which are transferred to the IVS and to the TLF. The magnitude of the nucleon transfer is generally not the same for the neutrons and for the protons. In peripheral collisions the N/Z ratio of the PLF and the TLF is nearly the same as of the P and T nuclei, respectively. For more central collisions the (N/Z)PLF increases and the (N/Z)TLF decreases. In consequence, the PLF loses more protons than neutrons, diverging from the stability line. In order to recompense this effect, more neutrons (neutron reach particles) than protons (proton reach particles) should be emitted from the excited primary PLF. For the TLF, one should observe the opposite effect. Unfortunately, in our experiment we were able to identify the Z of the emitted intermediate mass fragments, but not the A.

This work was supported by the Polish State Committee for Scientific Research (KBN) Grant no. PB 1188/ P03/ 98/ 14) and the M.Skłodowska-Curie Fund (MEN/DOE- 97-318).

REFERENCES

[1] See for example, A.J. Cole, *Statistical Models for Nuclear Decay*, Fundamental and Applied Nuclear Physics Series, Institute of Physics Publishing, Bristol and Philadelphia 2000; K. Grotowski, *Acta Phys. Pol.* **B31**, 253 (2000).

[2] See for example, W.U. Schröder, J.R. Huizenga, in *Treatise on Heavy-Ion Science*, D.A. Bromley, Editor, Plenum Press, New York and London, 1984, Vol. 2, pp. 113–726.

[3] L. Stuttgé *et al.*, *Nucl. Phys.* **A539**, 511 (1992); B. Lott, *et al.*, *Phys. Rev. Lett.* **68**, 3141 (1992).

[4] See B. Borderie *et al.*, *Phys. Lett.* **B205**, 26 (1988); W.U. Schröder, *Nucl. Phys.* **A538**, 439c (1992); Z. Sosin *et al.*, *Nucl. Phys.* **A574**, 474 (1994).

[5] J. Péter *et al.*, *Nucl. Phys.* **A593**, 95 (1995).

[6] W.J. Świątecki, *Phys. Scr.* **24**, 113 (1981); O. Mazonka, C. Jarzyński, J. Błocki, *Nucl. Phys.* **A641**, 335 (1998).

[7] J. Błocki *et al.*, *Ann. Phys.* **113**, 330 (1978).

[8] L.G. Sobotka, *Phys. Rev.* **C50**, R1272 (1994).

[9] P. Pawłowski *et al.*, *Phys. Rev.* **C57**, 1771 (1998).

[10] M. Colonna, M. Di Toro, A. Guarnera, V. Latora, A. Smerzi, Z. Jiquan, *Nucl. Phys.* **A583**, 525 (1995).

[11] E. Plagnol *et al.*, *Phys. Rev.* **C61**, 014606 (2000).

[12] Z. Sosin *et al.*, *Eur. Phys. J.*, paper II, **A11**, 305 (2001).

[13] J. Töke *et al.*, *Nucl. Phys.* **A583**, 519 (1995).

[14] J.F. Dempsey *et al.*, *Phys. Rev.* **C54**, 1710 (1996).

[15] T. Lefort *et al.*, *Nucl. Phys.* **A662**, 397 (2000).
[16] D. Dore *et al.*, *Phys. Lett.* **B491**, 15 (2000).
[17] F. Bocage *et al.*, *Nucl. Phys.* **A676**, 391 (1999).
[18] P. Pawłowski *et al.*, *Eur. Phys. J.* **A9**, 371 (2000).
[19] R. Płaneta *et al.*, *Eur. Phys. J.*, paper I, **A11**, 297 (2001).
[20] Z. Sosin, *Eur. Phys. J.*, paper III, **A11**, 311 (2001).
[21] D. Drain *et al.*, *Nucl. Instrum. Methods Phys. Res., Sect. A* **281**, 528 (1989).
[22] T. Barczyk *et al.*, *Nucl. Instrum. Methods Phys. Res., Sect. A* **364**, 311 (1995).
[23] P. Pawłowski *et al.*, *Z. Phys.* **A357**, 387 (1997).
[24] R.J. Charity *et al.*, *Nucl. Phys.* **A483**, 371 (1988).
[25] L. Tassan-Got, C. Stéphan, *Nucl. Phys.* **A524**, 121 (1991).
[26] see P.J. Karol, *Phys. Rev.* **C11**, 1203 (1975).
[27] M.E. Brandan *et al.*, *Nucl. Instrum. Methods Phys. Res., Sect. A* **334**, 461 (1993).
[28] see *e.g.* R. Płaneta *et al.*, *Phys. Rev.* **C39**, 1197 (1989).